MECHANISMS OF AGGLOMERATION IN FLUIDIZED BED: REACTIONS BETWEEN POTASSIUM CARBONATE AND SILICA

Bozidar Anicic[1,2], Weigang Lin[1], Hao Wu[1], Kim Dam-Johansen[1],

[1]*Department of Chemical and Biochemical Engineering, Technical University of Denmark, Søltofts Plads, Building 229, Kongens Lyngby, Denmark*

[2]*Sino-Danish Centre for Education and Research, Zhongguancun East Road 80, Beijing, China*

Abstract: Agglomeration is one of the main operational problems in fluidized bed combustion of biomass. Agglomeration is induced by interaction between the potassium species present in biomass and the bed materials (i.e. silica sand). To understand agglomeration mechanisms in biomass combustion, mixtures of model potassium compounds (KCl, K_2SO_4 and K_2CO_3) and silica sand were tested in bench scale fluidized bed reactors indicating that only potassium carbonate is able to react with the silica sand particles forming low melting point potassium silicates. The objective of this work is to reveal the reaction mechanism between K_2CO_3 and silica sand, which can be an important step in understanding overall agglomeration mechanism in fluidized bed combustion of biomass. The results indicate that the reaction between K_2CO_3 and silica sand occurred in solid-solid phase with reasonably high reaction rate under fluidized bed combustion temperature (> 800 °C). The initial reaction stage is dominated by surface diffusion of the salt molecules invading fresh silica sand surface, followed by the formation of a thin product layer. The reaction further proceeds by diffusion through the formed product layer. The reaction rate is dependent on temperature, CO_2 partial pressure, particle size and mixing of the reactants. The experimental data obtained in this work provide a basis for further modeling of the agglomeration process in fluidized bed combustion of biomass.

INTRODUCTION

Fluidized bed combustion is a promising technology for utilization of biomass for heat and power production (Khan et al. 2009). The technology offers good heat and mass transfer, fuel flexibility and high combustion efficiency (Grimm et al. 2011; Bartels et al. 2009; Loo et al. 2002). One of the challenges associated with fluidized bed combustion of biomass is agglomeration, which can influence hydrodynamics of the boiler, and in severe cases cause bed defluidization, leading to unscheduled shutdown of the plant (Gatternig & Karl 2016; Elled et al. 2013; Nuutinen et al. 2004).

Bed agglomeration primarily results from the presence of liquid on the surface of bed materials. In biomass combustion, it is commonly agreed that agglomeration is caused by the interactions between the alkali species, mainly potassium species from biomass and the bed materials (e.g. silica sand) (Lin et al. 2003; Gatternig and Karl 2016; Scala and Chirone 2008; Brus et al. 2005). During combustion, the potassium species present in biomass can be released to gaseous phase (e.g. as KCl) or retained in ash (e.g. as potassium silicates). Investigations showed that between 20 and 45 % of potassium is released primarily via KCl vaporization during combustion of annual biomass below 800 °C. (Knudsen el al. 2004). The presence of KCl in biomass ash is confirmed by several studies using XRD analysis of biomass ash (Umamaheswaran & Batra 2008; Thy et al. 2013; Wang et al. 2012; Boström et al. 2012). The amount of potassium released in the form of KCl will be lower for fuels with lower Cl/K ratio, and the remaining potassium will be released at higher temperatures via formation of different K-species. It is suggested that K release at higher temperatures may be associated with decomposition of different potassium salts such as K_2CO_3 and K_2SO_4 (Knudsen et al. 2004). K_2SO_4 has been found in the ashes obtained from combustion of straw and wood (Xiao et al. 2011;Olanders and Steenari 1995). The formation of K_2CO_3 has been suggested in several thermodynamic studies (Boström et al. 2012; Johansen et al. 2011; Wei et al. 2005) and K_2CO_3 was detected by XRD analysis in the fly ash obtained from a pulverized wood-fired power plant (Wu et al. 2013). Umamaheswaran et al. (2008) detected K_2CO_3 in the ash obtained from groundnut shell combustion below 650 °C. Zhao et al. (2015) proposed formation of a significant amount of K_2CO_3 in char from fast pyrolysis of rice husk in the temperature range 500–900 °C, based on the amount of water soluble potassium and anions (SO_4^{2-}, PO_3^{3-}, HCO^{3-}) detected. The potassium retained in the ash is mainly in a form of amorphous potassium silicates (Skrifvars et al. 2005; Piotrowska et al. 2010).

Sevonius et al. (2013) studied the reaction between model salts (KCl, K_2CO_3, K_2SO_4) and silica sand in a lab scale fluidized bed in the temperature range from 750–900 °C. Defluidization occurred in the case of KCl and K_2CO_3 addition, while no bed agglomeration was observed in the case of K_2SO_4 addition. KCl did not react with silica sand but acted as a glue agent binding bed particles, while K_2CO_3 reacted with silica sand forming a molten phase responsible to the bed agglomeration (Sevonius et al. 2013). Narayan et al. (2016) performed the similar study in a lab scale fluidized bed, where model salts (KCl and K_2CO_3) were added to silica sand to investigate the defluidization temperature. The addition of KCl caused defluidization in the temperature range 756-765 °C, while the K_2CO_3 addition caused defluidization between 728-737 °C. SEM-EDX analysis revealed that KCl did not react with silica sand, while K_2CO_3 reacted with silica sand forming high viscous potassium silicates.

These results indicate the importance of investigating the reaction mechanism between K_2CO_3 and silica sand. To the authors knowledge, only Arvelakis et al. (2004) briefly studied the reaction between K_2CO_3 and silica sand using simultaneous thermal analysis observing significant mass loss from 700 °C to 1100 °C under a heating rate of 10 °C /min. On the other hand, the mass loss associated with decomposition of K_2CO_3 starts at approximately 900 °C. These results indicate that reaction between K_2CO_3 and silica sand actually occurs and a systematic investigation of the reaction is yet not available.

In this paper, a systematical investigation on the reaction mechanism between K_2CO_3 and silica sand was performed. The influence of key parameters, such as reaction temperature, gas environment (CO_2 partial pressure), mixing, and particle size was examined. The agglomerate samples were analyzed by using SEM-EDX in order to reveal the reaction mechanisms.

EXPERIMENTAL

Materials

Potassium carbonate (CAS 584-08-7) was purchased from Sigma Aldrich and was pulverized into two sizes with mean diameters of 18 µm (hereafter denoted as powder K_2CO_3) and 285 µm (hereafter denoted as coarse K_2CO_3), respectively. The silica sand particles have a mean diameter of 385 µm, corresponding to the typical size used in fluidized bed boilers. The sand was pretreated at 800 °C under oxidizing conditions for 2h to remove the organic impurities.

Total amount of the sample was 0.7 g approximately, corresponding to the crucible filling limit. Mixing of the particles was carried out manually (intensively mixed for 10 minutes) in a crucible, which is further used in the thermogravimetric analyzer. Besides well-mixed samples, two types of segregate samples were also prepared. Firstly, the bottom of crucible was filled with sand, and salt was placed above it, completely covering the upper sand surface (the salt/sand ratio was approximately equal to 3:100 w/w). The procedure was similar for preparation of second segregate sample, but in this case the salt was only localized at the middle of the upper sand surface.

Thermogravimetric analysis

The K_2CO_3/silica sand system was studied using a thermogravimetric analyzer (TGA) *Netzsch STA 449 F1 Jupiter,* which measures the mass change of a sample under a specified temperature program and gas environment. The salt conversion was quantified by monitoring the mass loss due to the release of CO_2. The conversion is calculated as ratio between the amount of CO_2 released (monitored by mass loss) and the theoretical amount of CO_2 present in K_2CO_3.

A schematic view of the TGA analyzer is illustrated in Figure 1. Samples were initially heated to 150 °C and held for 1h in order to remove the moisture. Afterwards, the samples were heated 500 K/min to a final temperature between 700 and 850 °C and held for 4h. To present the TGA results, the initial time is chosen to be the time when the final, isothermal, temperature is reached. It is reasonable to expect that the value of initial conversion is increasing as temperature increases, meaning that reaction can occur even before the final temperature is reached. That is why; a high heating rate of 500 K/min was used. The gas used in the TGA included pure N_2, pure CO_2 and a mixture of 50% CO_2 and 50% N_2. The gas flow rate was set to 50 mL/min.

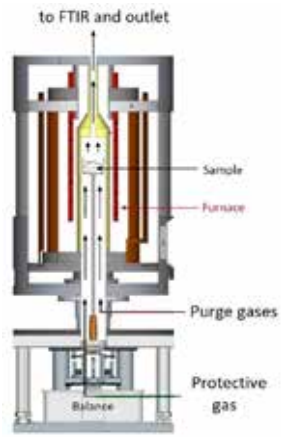

Figure 1: Cross sectional view of the TGA analyzer.

Agglomerate samples analysis

The solid samples obtained from the experiments were analyzed using a Scanning Electron Microscopy combined with Energy dispersive X-ray (SEM-EDX) analysis (*JEOL JSM-5910*), and X-ray diffraction analysis (XRD).

RESULTS

Influence of the key reaction parameters

The influence of the different operating parameters on the conversion of K_2CO_3 was evaluated. The impact of reaction temperature, mean particle size, gas atmosphere and mixing is examined. Figure 2 shows the K_2CO_3 conversion history under different operating conditions.

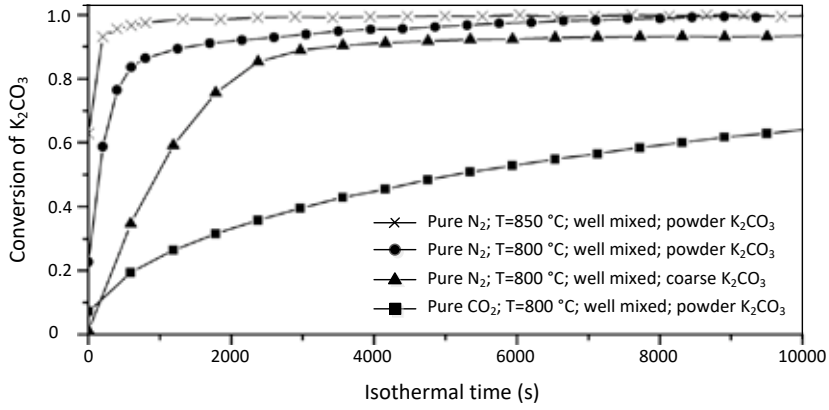

Figure 2: K_2CO_3 conversion as a function of isothermal time under different operating conditions. SiO_2 to K_2CO_3 mass ratio is 100:3 in all experiments.

The results generally show that the reaction is sensitive to temperature, and that K_2CO_3 will be almost completely converted regardless the temperature with sufficiently long residence time. At 850 °C, the K_2CO_3 was fully converted within a few minutes, and a considerable conversion of K_2CO_3 is achieved before the isothermal phase is reached. Furthermore, the influence of the particle size is significant at initial stages of reaction. Only the results obtained at 800 °C are presented here, but the impact of the particle size is even more significant at lower temperatures. At 850 °C and 800 °C, complete conversion of powder K_2CO_3

particles is achieved regardless the operating temperature. However, coarse K_2CO_3 particles only reach a final conversion around 0.9 at 800 °C. The results suggest that impact of K_2CO_3 particle size is significant, both for the conversion rate and the final conversion degree, and the effect is more pronounced at lower temperatures. Moreover, the influence of the gas environment is evaluated by performing experiments under different atmosphere. Figure 2 shows that the conversion of K_2CO_3 at 800 °C is strongly inhibited by the presence of CO_2. The initial conversion rate is much slower, and final conversion degree is lower under pure CO_2 atmosphere. Experiments performed under mixed atmosphere (50 % of N_2, 50 % of CO_2) revealed that the difference between 50% CO_2 and 100% CO_2 is not significant, especially at initial stage.

The influence of mixing was investigated by analyzing aforementioned segregated (two phase) mixtures. Figure 3 shows the conversion of K_2CO_3 for different mixtures. The results suggest that initial conversion rate is significantly impacted by the mixing; meaning that conversion of K_2CO_3 is strongly reduced for segregated mixtures. A segregated sample where salt particles cover complete silica sand surface eventually reaches complete conversion under sufficient residence time. On the other hand, the final conversion for the sample with localized K_2CO_3 is significantly lower compared to the other two mixtures due to the limited contact area between reactants.

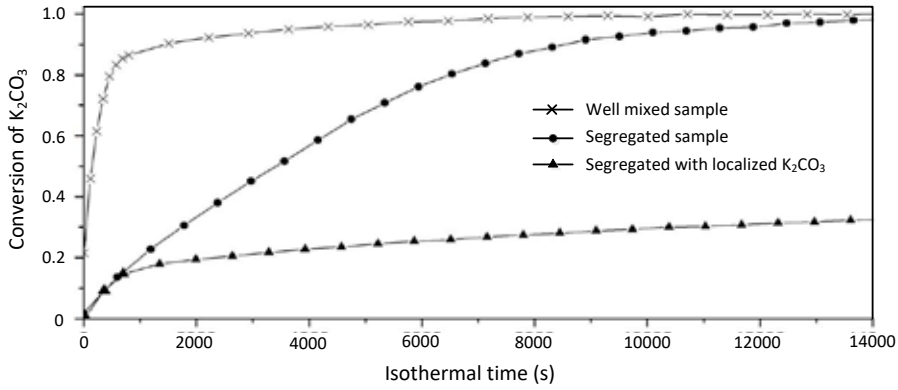

Figure 3: Conversion rate for different mixtures. T = 800 °C; Pure N_2; K_2CO_3:SiO_2 ratio = 3:100; powder K_2CO_3; total residence time 4h.

SEM-EDX analysis

SEM-EDX analysis of the reaction products was performed to understand the reaction mechanism. Typical results of SEM-EDX analysis is presented on Figure 4. The sample obtained from segregated mixture under CO_2 atmosphere is shown since the salt is not completely converted (final conversion was 0.25) and reaction propagation can be clearly observed. Spot 1 in Figure 4 shows unreacted K_2CO_3, while Spot 2 represents a layer of potassium silicate covering the silica sand surface. Finally, Spot 3 represents unreacted silica sand surface. Figure 4 indicates that reaction can proceed away from initial contact points of K_2CO_3 and silica sand, since the formed potassium silicate invades the unreacted silica surface. On the other hand, it seems that at the current conditions, the invasion is limited to certain extent since not the complete sand surface is covered by the product layer, even though potassium carbonate is still present in the system.

Several agglomerated samples were imbedded in epoxy resin and gradually polished in order to observe cross section of agglomerated silica sand grains. A SEM image of one of imbedded samples is presented in Figure 5 together with the mapping along the whole sample area as well as elemental analysis along the line. The sample was prepared at 850 °C under N_2 atmosphere, while the ratio between powder K_2CO_3 and silica sand was 3:100. The salt was fully converted under mentioned conditions.

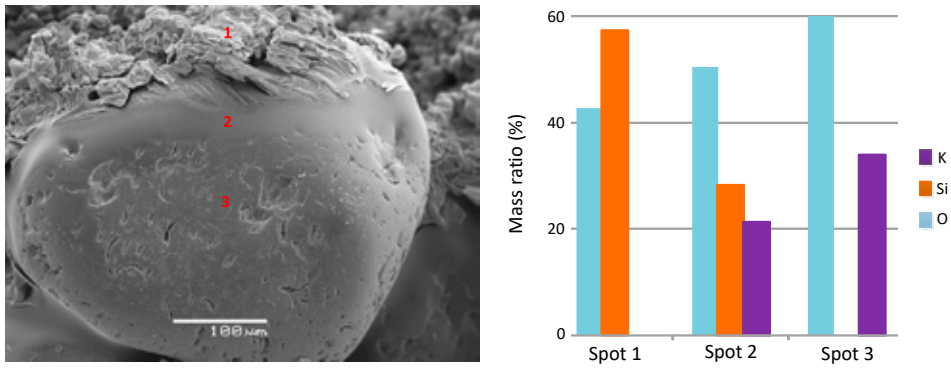

Figure 4: SEM-EDX analysis of a representative reaction product: SiO_2:K_2CO_3 ratio = 3:100; T= 800 ºC; pure CO_2 atmosphere; segregated mixture; powder form of K_2CO_3; isothermal reaction time 4h.

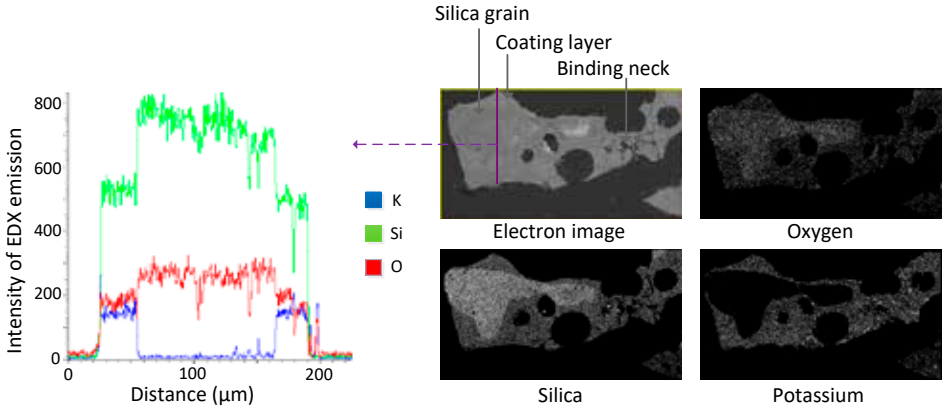

Figure 5: SEM-EDX analysis of imbedded samples. SiO_2:K_2CO_3 ratio = 3:100; T= 850 ºC; pure N_2 atmosphere; well mixed sample; powder form of K_2CO_3; isothermal reaction time 4h.

It can be clearly observed that silica grain is covered by a continuous product layer with varying thickness, probably due to the different initial local K_2CO_3 concentration. The layer acts as a binding neck to connect two silica grains, as indicated at Figure 5. The elemental analysis along the line reveled that both silica and potassium are present in the product layer. Both elements are distributed equally along the product layer indicating formation of a homogeneous layer. A sharp concentration change of Si and K is observed at the interface between the layer and silica grain, which further proves the formation of a homogeneous layer without the presence of an intermediate phase. The obtained results are similar as SEM-EDX analysis of agglomerated samples from straw combustion in lab scale fluidized bed, where formation of continuous product layer covering silica sand surface and acting as a binder of grains was observed (Lin et al. 2003). Furthermore, Lin et al. (2003) observed steep potassium concentration profile at the interphase between the layer and the grain, and concluded that the formation of this layer is main reason for sand particles agglomeration.

DISCUSSION

Plausible reaction mechanism

The reaction between K_2CO_3 and silica sand starts at the contact point resulting in formation of potassium silicate, which occurs either in solid or high viscous liquid form (under investigated conditions). Initial stage of reaction is schematically presented in Figure 6.

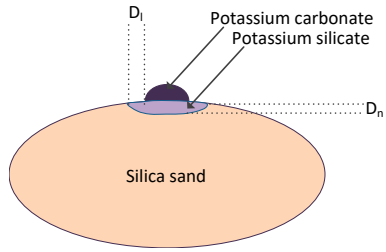

Figure 6: Schematic representation of initial stage of reaction between K_2CO_3 and silica sand

The reaction can proceed in two directions: toward the silica sand interior and on the silica sand surface. The distances, D_l (lateral) and D_n (normal), are distances from the source of potassium (K_2CO_3). Analysis of conversion curve of the segregated sample containing localized K_2CO_3 (Figure 3) revealed that clear conversion change occurred after conversion reached approximately 20 % indicating termination of initial conversion rate. Such observation can be explained by assumption that the surface diffusion (lateral growth) is a dominant mechanism at initial reaction stages and the assumption can be supported by the SEM-EDX analysis of the sample represented at Figure 4. The number of powder K_2CO_3 particles is much higher compared to the number of silica sand particles (1000000:1 ratio), meaning that significant number of K_2CO_3 particles will be initially adhered to the surface of each silica sand grain. The surface (lateral) diffusion and associated reaction will lead to the formation of product coating layer before the limiting distance is reached. That is the reason why the significant conversion rate change is observed only for segregated sample with localized K_2CO_3, and for all the others the transition from surface diffusion mechanism to normal growth is not so obvious.

Afterwards, the reaction proceeds by the diffusion through the formed product layer. The amount of K_2CO_3 that remained unreacted after the formation of product layer depends on the size of the salt particles as well as on its content in the mixture. The diffusion through formed product layer can be explained using two plausible mechanisms. The first mechanism includes diffusion of potassium carbonate through the product layer and its reaction with silica sand once it reaches sand surface. One the other hand, the second reaction mechanism assumes formation of silicates with the different potassium/silica ratio. Initial formed potassium silicate may further react with both, fresh silica sand or non-reacted potassium carbonate, which results in formation of the different silicates at different reaction time. Unfortunately, all of the formed products are amorphous; therefore its detection using XRD analysis is not possible, since the only crystalline phase detected was silica sand. The SEM-EDX analysis of imbedded samples can provide elemental composition in the formed product layer, which may furthermore reveal formation of different potassium silicates. The evaluation of described reaction mechanisms will be done in the future by preparing samples with different residence time.

Impact of operating parameters

Some of the investigated parameters have impact on the overall reaction rate, while other influence more either initial conversion rate (surface diffusion controlled) or the later reaction stage (diffusion through product layer). Number of initial contact points is an important parameter directly influencing the initial K_2CO_3 conversion rate, as well as indirectly affecting later stages of reaction. The formation of continuous product layer is faster for the higher number of initial contact points. The total number of the contact points depends on mixing and particles size of reactants. That is why; the initial conversion rate of samples containing powder K_2CO_3 and of well-mixed samples is much higher compared to the samples containing coarse K_2CO_3 or segregated mixtures, respectively. Besides that, number of initial contact points influences

the amount of K_2CO_3 that will be converted in the initial stage, as well as the thickness of the formed product layer. The layer thickness will be much higher for the samples containing coarse K_2CO_3. After the limiting lateral distance is reached or the continuous product layer is formed, the only way of K_2CO_3 transport to the non-reacted silica sand surface will be diffusion through formed product layer. The diffusion of the non-reacted K_2CO_3 can be terminated due to the diffusion layer thickness. This may explain that some amount of coarse K_2CO_3 remained non-converted even after 4h (final conversion of coarse K_2CO_3 at 800 °C is 0.9).

The impact of system temperature can be clearly observed from Figure 2. Temperature increase promotes overall K_2CO_3 conversion rate. Obtained results are consistent with well-known Arrhenius equation, where reaction rate constant increase is correlated to the temperature increase. On the other hand, system temperature can change physical properties of the formed products, thus influencing overall reaction mechanism. The temperature increase may result in formation of phase with lower viscosity, thus enhancing particle wetting and the impact of gravitational force in the initial stage of product layer formation consequentially leading to the formation of the evenly distributed product layer. The temperature impact on the overall reaction mechanism will be evaluated after mentioned SEM-EDX analysis of imbedded samples as well as after performing comprehensive thermodynamic calculation. These analyses will give us information about possible silicate formation, thus enabling us to obtain information about physical properties of formed silicates.

Finally, performed experiments showed that impact of CO_2 is significant and its presence strongly inhibits the salt conversion rate, which indicates that CO_2 plays an important role in the overall reaction mechanism. Comparable impact of the CO_2 is observed in the similar, sodium carbonate/silica sand system (Gibsont & Ward 1943; Grynberg et al. 2015). Gibsont & Ward (1943) suggested that carbonate ions actively participate in breakage of long silicon chains and formation of silicon ions suitable for attachment of alkali metals. They also suggested that desorption of CO_2 from the reaction surface is very important step in the overall reaction mechanism. The CO_2 desorption rate is influenced by CO_2 presence in the atmosphere, which can explain the overall reaction rate reduction under these operating conditions.

CONCLUSIONS

The results of this work indicate that reaction between K_2CO_3 and silica sand may occur in solid-solid phase with reasonably high reaction rate under fluidized bed combustion temperature (> 800 °C). The reaction between those species occurs in two stages. The initial stage is dominated by surface diffusion of the salt molecules invading fresh silica sand surface. This will lead to formation of thin product layer. The reaction proceeds by diffusion through the formed product layer and it may result in formation of high viscous molten phase completely covering the silica sand surface. The reaction rate is dependent on system temperature, reactants particle size, CO_2 partial pressure, and mixing. The experimental data obtained in this work provide a basis for understanding and evaluating of agglomeration process in fluidized bed combustion of biomass.

ACNOWLEDGMENT

This project is funded by Innovation Fund Denmark (DANCNGAS), Sino-Danish Center for Education and Research, and Technical University of Denmark.

REFERENCES

Arvelakis, S., Jensen, P. A., Dam-Johansen, K. (2004). Simultaneous Thermal Analysis (STA) on Ash from High-Alkali Biomass. Energy & Fuels, *18*(4), 1066–1076.

Bartels, M., Nijenhuis, J., Lensselink, J., Siedlecki, M., de Jong, W., Kapteijn, F., van Ommen, J. R. (2009). Detecting and Counteracting Agglomeration in Fluidized Bed Biomass Combustion. Energy & Fuels, *23*(1), 157–169.

Boström, D., Skoglund, N., Grimm, A., Boman, C., Öhman, M., Broström, M., Backman, R. (2012). Ash Transformation Chemistry during Combustion of Biomass, Energy and Fuels *26*(1), 85–93.

Brus, E., Öhman, M., Nordin, A. (2005). Mechanisms of Bed Agglomeration during Fluidized-Bed Combustion of Biomass Fuels. Energy & Fuels, *19*(3), 825–832. J

Elled, A.-L., Åmand, L.-E., Steenari, B.-M. (2013). Composition of agglomerates in fluidized bed reactors for thermochemical conversion of biomass and waste fuels: Experimental data in comparison with predictions by a thermodynamic equilibrium model. Fuel, *111*, 696–708.

Gatternig, B., Karl, J. (2016). Investigations on the Mechanisms of Ash-Induced Agglomeration in Fluidized-Bed Combustion of Biomass. *ENERGY & FUELS*, *29*(2), 931–941.
Gibsont, G., Ward, R. (1943). REACTIONS IN SOLID STATE: 111, REACTION BETWEEN SODIUM CARBONATE AND QUARTZ*. Journal of the American Ceramic Society, *26*(7), 239–246.
Grimm, A., Skoglund, N., Bostrom, D., Ohman, M. (2011). Bed Agglomeration Characteristics in Fluidized Quartz Bed Combustion of Phosphorus-Rich Biomass Fuels. *ENERGY & FUELS*, *25*(3), 937–947.
Grynberg, J., Gouillart, E., Chopinet, M.-H., Toplis, M. J. (2015). Importance of the Atmosphere on the Mechanisms and Kinetics of Reactions Between Silica and Solid Sodium Carbonate. International Journal of Applied Glass Science, *6*(4), 428–437.
Johansen, J. M., Jakobsen, J. G., Frandsen, F. J., Glarborg, P. (2011). Release of K, Cl, and S during Pyrolysis and Combustion of High-Chlorine Biomass. Energy & Fuels, *25*(11), 4961–4971.
Khan, A. A., de Jong, W., Jansens, P. J., Spliethoff, H. (2009). Biomass combustion in fluidized bed boilers: Potential problems and remedies. Fuel Processing Technology, *90*(1), 21–50.
Knudsen, J. N., Jensen, P. A., Dam-Johansen, K. (2004). Transformation and Release to the Gas Phase of Cl, K, and S during Combustion of Annual Biomass. Energy & Fuels, *18*(5), 1385–1399.
Lin, W., Dam-Johansen, K., Frandsen, F. (2003). Agglomeration in bio-fuel fired fluidized bed combustors. *Chemical Engineering Journal*, *96*(1), 171–185.
Loo, S. van (Sjaak), Koppejan, J.. Task 32: Biomass Combustion and Co-Firing. (2002). *Handbook of biomass combustion and Co-firing*. Twente University Press.
Narayan, V., Jensen, P. A., Henriksen, U. B., Glarborg, P., Lin, W., Nielsen, R. G. (2016). Defluidization in fluidized bed gasifiers using high-alkali content fuels. Biomass and Bioenergy, *91*, 160–174.
Nuutinen, L. H., Tiainen, M. S., Virtanen, M. E., Enestam, S. H., Laitinen, R. S. (2004). Coating Layers on Bed Particles during Biomass Fuel Combustion in Fluidized-Bed Boilers. Energy & Fuels, *18*(1), 127–139.
Olanders, B., Steenari, B.-M. (1995). Characterization of ashes from wood and straw. Biomass and Bioenergy, *8*(2), 105–115.
Piotrowska, P., Zevenhoven, M., Davidsson, K., Hupa, M., Åmand, L.-E., Barišić, V., Coda Zabetta, E. (2010). Fate of Alkali Metals and Phosphorus of Rapeseed Cake in Circulating Fluidized Bed Boiler Part 1: Cocombustion with Wood. Energy and Fuels, *24*(1), 333–345.
Scala, F., Chirone, R. (2008). An {SEM}/{EDX} study of bed agglomerates formed during fluidized bed combustion of three biomass fuels. Biomass and Bioenergy, *32*(3), 252–266.
Sevonius, C., Yrjas, P., Hupa, M. (2013). Defluidization of a quartz bed – Laboratory experiments with potassium salts. Fuel, *127*.161-168.
Skrifvars, B.-J., Yrjas, P., Kinni, J., Siefen, P., Hupa, M. (2005). The Fouling Behavior of Rice Husk Ash in Fluidized-Bed Combustion. 1. Fuel Characteristics. Energy and Fuels, *19*(4), 1503–1511.
Thy, P., Yu, C., Jenkins, B. M., & Lesher, C. E. (2013). Inorganic Composition and Environmental Impact of Biomass Feedstock. Energy and Fuels, *27*(7), 3969–3987.
Umamaheswaran, K., Batra, V. S. (2008). Physico-chemical characterisation of Indian biomass ashes. Fuel, *87*(6), 628–638.
Wang, G., Shen, L., Sheng, C. (2012). Characterization of Biomass Ashes from Power Plants Firing Agricultural Residues. Energy & Fuels, *26*(1), 102–111.
Wei, X., Schnell, U., Hein, K. R. G. (2005). Behaviour of gaseous chlorine and alkali metals during biomass thermal utilisation. Fuel, *84*(7), 841–848.
Wu, H., Bashir, M. S., Jensen, P. A., Sander, B., Glarborg, P. (2013). Impact of coal fly ash addition on ash transformation and deposition in a full-scale wood suspension-firing boiler. Fuel, *113*, 632–643.
Xiao, R., Chen, X., Wang, F., Yu, G. (2011). The physicochemical properties of different biomass ashes at different ashing temperature. Renewable Energy, *36*(1), 244–249.
Zhao, H., Song, Q., Wu, X., Yao, Q. (2015). Study on the Transformation of Inherent Potassium during the Fast-Pyrolysis Process of Rice Straw. Energy & Fuels, *29*(10), 6404–6411.